34th Annual International Conference of the IEEE EMBS
San Diego, California USA, 28 August - 1 September, 2012

CHIC: Cylindrical Helix Imaging Coordinate Registration Fiducial for MRI-Guided Interventions

Yunzhao Ma*, Ivo Dobrev*, Weijian Shang, Hao Su, Satyanarayana Reddy Janga and Gregory S. Fischer

Abstract—**Accurate placement of tubular shaped surgical tools is necessary for a large variety of image-guided medical interventions. In this process, localization of the instrument, or a robotic assistant manipulating the instrument, is crucial for successful registration of physical space to medical image space. Various fiducial frames and registration methods have been proposed and discussed in literature. However, these frames are typically bulky in size or otherwise not appropriate for use with MR imaging. In particular, it is impossible or awkward to integrate them with the surgical tools. This paper presents the design a compact Cylindrical Helix Imaging Coordinate Registration Fiducial (CHIC) and algorithm to precisely and robustly localize the frame in 6 degree of freedom (DOF). The mathematical model of the frame is developed and evaluated with simulation. This cylindrical shaped frame is particularly suitable for mounting to the distal end of tubular shape surgical tools, which provides a direct imaging visualization of frame, tool and possibly the surgical sites. The paper uses MRI-guided surgical procedure as a focusing application, although the broader aim is development of a versatile registration frame that is usable for a variety of image-guided procedures ranging from ultrasound to fluoroscopy and computerized tomography (CT). Accuracy and performance were evaluated in three cases: simulated images with artificial noise, arbitrarily re-sliced 3D MRI volume, and real 3T MRI images.**

I. Introduction

The last decade witnessed rapid development of cancer treatment technologies. Tubular shaped surgical tools, ranging from needles, stimulators, shunts, aspirators, to ablators and drills, are often inserted or placed into human body cavities or tissues in many minimally invasive surgeries. However, the efficiency of these treatments often heavily depends of the accurate and effective administering of the treatment. In many cases, the physical delivery of therapy to the tumor is inherently a stereotactic problem such as deep brain stimulation [1] and prostate intervention [2]. Therefore, effective image guided methods are needed to facilitate the accurate delivery of therapy.

Robot-assisted surgical interventions have been evolving from early laboratory development to wide clinical applications with increased targeting accuracy. Surgical robots, combined with MRI guidance whose high soft-tissue contrast can be taken advantage of, are becoming more typical tools for real time guidance. However, it is crucial to know the position and orientation of the surgical tool relative to the patient anatomy, intraoperative imaging, and surgical plan. This is typically determined using objects and features with known geometry that can be imaged in the MRI – referred to as fiducial frames.

*Shared first authorship.
Yunzhao Ma, Weijian Shang, Ivo Dobrev, Hao Su, Satyanarayana Reddy Janga and Gregory S. Fischer, are with the Automation and Interventional Medicine (AIM) Laboratory in the Department of Mechanical Engineering at Worcester Polytechnic Institute, Worcester, MA, USA. gfischer@wpi.edu

A wide variety of registration and tracking approaches have already been shown including using active coils, encoders and passive fiducials [3]. High accuracy and tracking speed have been found in methods using active tracking coils. Some of them have been discussed by Krieger [3], Derbyshire [4] and Hillenbrand [5]. But the requirement of special scanner programming, limitations of scanner channel and special design of electronic hardware [3] are potentially significant disadvantages to these methods.

Compared to using active tracking coils, registration and tracking by using passive fiducials does not require complicated equipment and imaging protocols. Several single- and multi-image approaches have been shown in prior works. Both passive single-image registration and tracking in MRI and CT environment have been discussed by DiMaio and Susil in [6,7]. To make the single image, 6-DOF registration more accurate, several numerical algorithms have been designed by Lee [8]. Alternatively, we have also developed high accuracy multi-image registration approaches using a similar fiducial frame by Shang [9].

Placing the fiducial frame as close to the end effector as possible will produce the best registration result since it could reduce lever effect. This scalable cylindrical shaped frame is particularly suitable for mounting to the distal end of tubular shape surgical tools, which provides a direct imaging visualization of frame, tool and possibly the surgical sites. Using a fiducial frame coaxial with the instrument avoids error from kinematics and control as much as possible. Most of the designs in the prior works are bulky in size and could only be integrated into a robot's base, thus not preventing calibration error to be introduced into tool localization. In this paper, a novel compact fiducial frame for registration of an MRI-compatible cannula placement robot is developed, and is design to minimize the physical size and maximize robustness and accuracy. Presented is a registration algorithm with mathematic model of Cylindrical Helix Imaging Coordinate (CHIC) fiducial.

II. Methods

A. Fiducial Design

The design of CHIC fiducial frame utilizes the depth detection technique that is similar to Brown-Roberts-Wells (Z-frame) [6,7] along with a higher density of tubular mesh similar to [10] for improved detection accuracy and stability of the detection algorithm. It incorporates an initial angular offset between the trajectories of the helix tubes so that they don't fully overlap at each end of cylinder – this allows for more reliable registration at the extreme pose of the target.

The detection process relies on machine vision based techniques for image processing to determine the pose (azimuth, elevation and twist angles from tilt cross-section relative to the fiducial plane) and the centroid of the elliptical cross-section as well as the positions of the centers of the each tube's cross-sections.

The unique feature for this design is that the pattern of the mesh allows direct detection of both depth and twist of the image with respect to the fiducial plane. The CHIC fiducial frame can be used to estimate the full 6-DOF parameter set for the arbitrary pose from a single cross-sectional image. The design shown in Fig. 1 utilizes:

- Four straight tubes as diametric markers to form a cruciate fiducial,
- Three sets of helix curves as axis position markers to provide depth information, and
- Two straight tubes to make the frame asymmetric for detecting twist angle and improving ellipse fitting.

The axial position markers utilize a typical cylindrical helix coordinate, where each helix tube has a predefined pitch along the relative quadrant between two straight fiducial tubes along the central axis.

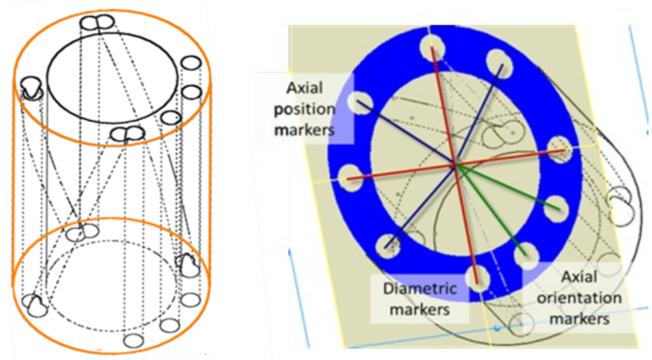

Figure 1. CHIC frame fiducial CAD model (left) and unique registration tubular mesh pattern (right). Axial position markers (blue lines) and diametric markers (red cross) to determine the depth along central axis, axis orientation marker (green angle) to determine the twist angle and all centroid of tubes were fitted into elliptical curve to determine the pose

In manufacturing the CHIC frame fiducial frame, the prototype consists of two parts: main body (height 50mm, external diameter 30mm, inner diameter 20mm, tube diameter 3mm, initial angular offset 10˚) that contains the registration tubular mesh pattern, and the caps that seal in the registration fluid. The tubes are filled with high MRI contrast liquid or gel. The module is made by 3D printing as shown in Fig. 2. The specific design is scalable and reconfigurable.

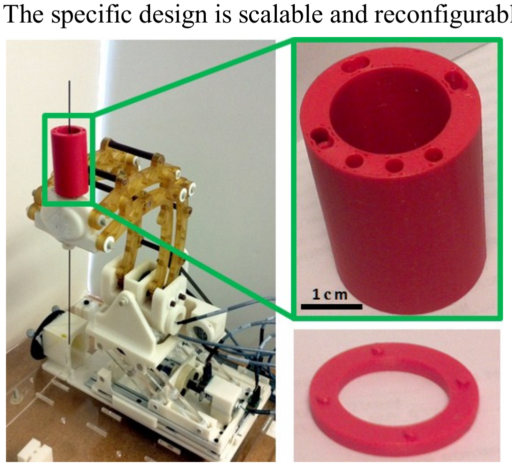

Figure 2. CHIC frame fiducial frame demonstrated on our stereotactic neurosugery robot [1] (left) and its construction before filling (right).

The proposed approach requires visualization of all tubular mesh cross-sections in the single cross-section. Therefore, the current prototype shown in Fig. 2 is limited to a tilt angle of 63.5˚ for a cross-section in the midpoint of the fiducial center axis and to approximately 30˚ in the central range of 35mm along the axis where spiral tubes don't touch cruciate tubes as shown in Fig. 3. However, this is a rather conservative constraint and a larger range of cross-section angles and positions along z-axis can be achieved by employing a curve fitting algorithm that establishes the best fit ellipse through confluent pair-points. Since MRI is a true 3D imaging modality, it is possible to ensure that the cross-section image is close to normal with the tool axis in most cases, and the scan plane can be updated based on fiducial orientation when a larger range of motion is anticipated.

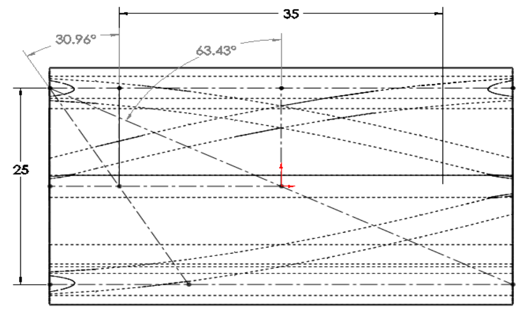

Figure 3. Lateral view of the CHIC fiducial frame showing limitations on the centroid estimation for this prototype configuration.

B. *Mathematic Model*

1. Coordination systems definitions

Registration is based on the coordinate system shown in Fig. 4. The coordinate system F_i is internally calibrated and related to the primary coordinate system of the fiducial F_f with certain displacement along central axis. The coordinate system of the cross-section F_c, which is homocentric with F_i and the X_c and Y_c axis are oriented along the two axis of the elliptical cross-section. The Z_c axis is normal vector to the plane of the cross-sectional image.

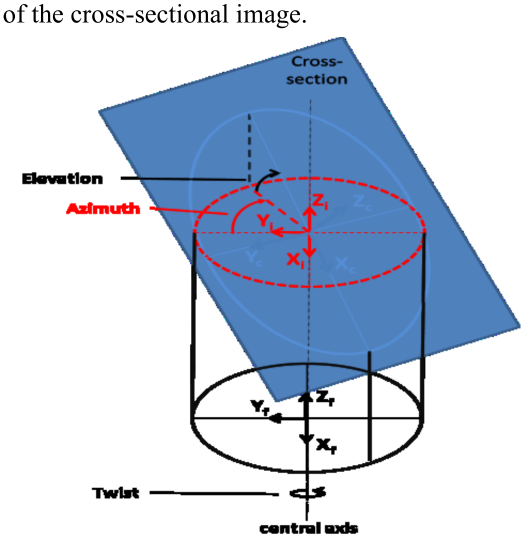

Figure 4. Coordinate systems in CHIC fiducial frame. F_f if the primary fixed frame of the fiducial, F_c is the aligned frame at the intersection of the image, and F_i is in the cross-sectional image.

2. Cross-section pose detection and ellipse reconstruction

The range of reliability of the cross-section pose detection is based on the range of reliability of the ellipse reconstruction, which in turn is dependent on the number and distribution of the detected points around the circumference of cylindrical tubular mesh pattern in the cross-section. The pattern of tubular mesh in CHIC frame fiducial provides very high robustness for ellipse reconstruction using a least square approach. It avoids two important types of ellipse detection errors: lack of point numbers and improper distribution. A least square best fit elliptical curve through all the registration points allows us to do an initial estimation on making F_c coincide with F_i. Notice that F_c and F_i are homocentric and Z_c axis is cross-section's normal vector with respect to F_i.

Pose is determined by the elevation and azimuth angles. The elevation angle a can be estimated based on the ratio of the minor and major semi axis of the ellipse. The azimuth angle is estimated based on the projection of the semi-major axis of the ellipse relative to the centroid of the ellipse which is obtained directly from fitting ellipse equation. The elevation angle is defined as follows:

$$\alpha_{elevation} = \cos^{-1}\left(\frac{r_{minor}}{r_{major}}\right) \tag{1}$$

3. Estimation of twist around the central axis

The last rotation pose of the cross-section in the F_i system is defined with the angles of rotation around central axis. This rotation angle is found by detecting the orientation of the angular position of the axis orientation marker based on its position relative to the diametric markers. This is done by converting the coordinates of the detected points from Cartesian system to rotational system centered at the centroid of the cross-section. Under the rotational system, we first sequence all points clockwise with an arbitrary starting point and then find three successive points whose total angle is 90˚ – these are the axis orientation makers – to mark as starting point. Based on that, we can find the relative angle of every point to every other point.

Using these we can then detect which quadrant of the coordinate system F_c contains a pair of markers: one axis orientation and one diametric. This provides sufficient information to establish an estimate for the amount of twist around central axis. This is the 5th DOF of cross-section.

Based on the angles described in section 2 and 3, the normal vector of the cross-section relative to F_i can be estimated as follows:

$$\begin{cases} Z_{c_x} = \sin\alpha_{azimuth} \cdot \sin\alpha_{elevation} \\ Z_{c_y} = -cos\alpha_{azimuth} \cdot \sin\alpha_{elevation} \\ Z_{c_z} = \cos\alpha_{elevation} = \frac{r_{minor}}{r_{major}} \end{cases} \tag{2}$$

4. Estimation of depth position along the central axis

In the final step, the position of the centroid of the cross-section along the central axis of the fiducial frame is estimated. We first transform the coordinates of axis orientation maker points from F_c to F_f, by transforming its rotating angles, which step 3 has done, to its depth displacement relative to F_f. This aligns F_c and F_f leaving only a translational offset along the central axis of the frame. Knowing each rotating angle's α_k between the *k* pair markers of axis orientation and diametric, their corresponding depth displacement z_k, along the central axis of the frame is:

$$z_k = \frac{\alpha_k - 2\varphi}{\omega_k} \qquad (k = 1, 2, 3) \tag{3}$$

where ω_k is the pitch of the helix that defines this tubular mesh in dimensions of angle/distance (degree/mm) and φ is an initial angular offset which is equal in the each end of the cylinder. This gives the (x, y, z) position of the three axial position markers in F_f. Based on these three points, the equation of the cross-section in F_f can be established as:

$$Ax + By + Cz + D = 0 \tag{4}$$

where A, B, C and D are defined as:

$$A = \left\|\begin{bmatrix} 1 & y_1 & z_1 \\ 1 & y_2 & z_2 \\ 1 & y_3 & z_3 \end{bmatrix}\right\| \quad B = \left\|\begin{bmatrix} x_1 & 1 & z_1 \\ x_2 & 1 & z_2 \\ x_3 & 1 & z_3 \end{bmatrix}\right\|$$
$$C = \left\|\begin{bmatrix} x_1 & y_1 & 1 \\ x_2 & y_2 & 1 \\ x_3 & y_3 & 1 \end{bmatrix}\right\| \quad D = \left\|\begin{bmatrix} x_1 & y_1 & z_1 \\ x_2 & y_2 & z_2 \\ x_3 & y_3 & z_3 \end{bmatrix}\right\| \tag{5}$$

Here, (x_1, y_1, z_1), (x_2, y_2, z_2) and (x_3, y_3, z_3) are the coordinates of the three axial position markers in F_f. These can be simplified for computational efficiency as:

$$\begin{aligned} A &= y_1 \cdot (z_2 - z_3) + y_2 \cdot (z_3 - z_1) + y_3 \cdot (z_1 - z_2) \\ B &= z_1 \cdot (x_2 - x_3) + z_2 \cdot (x_3 - x_1) + z_3 \cdot (x_1 - x_2) \\ C &= x_1 \cdot (y_2 - y_3) + x_2 \cdot (y_3 - y_1) + x_3 \cdot (y_1 - y_2) \\ -D &= x_1 \cdot (y_2 \cdot z_3 - y_3 \cdot z_2) + x_2 \cdot (y_3 \cdot z_1 - y_1 \cdot z_3) \\ &\quad + x_3 \cdot (y_1 \cdot z_2 - y_2 \cdot z_1) \end{aligned} \tag{6}$$

Then bring the 2D central point of ellipse from step 2 into 3D plane equation to obtain its depth displacement in F_f. This is the last DOF of cross-section providing full 6-DOF localization. This also defines a normal vector to the plane in the direction of Z_c. This provides a second approach for verification of the pose angles of the cross-section defined previously. But since it is fitted from only three points, this approach has relatively low accuracy as compared with the ellipse equation which considers all 9 points in frame.

III. Results

A. Performance of the Registration Algorithm

The algorithm is capable of removing typical noise in MRI images, find the tubular mesh of cross-sections, and estimate the location of its centroids in image coordinate system. The algorithm was first tested to detect cross-section positions of the tubular mesh of simulated MRI images made from CAD model cross-sections as shown in Fig. 5. Artificially created uniformly distributed white noise was added and the filtration capabilities of the registration algorithm were adjusted and tested. The filtration algorithm applies a combination of thresh-holding, erosion, filling and feature area based filtration all done on BW images – total processing time is less than 10ms. The algorithm determines the 6-DOF pose and orientation of the cross-section and provides a normal vector along the central axis of the frame.

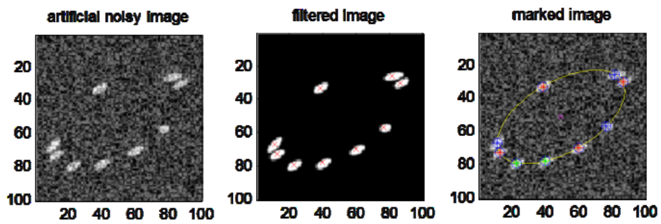

Figure 5. Simulated images with artificial noise (left), noise filtered (center) and localization and classification of the tubes' centroids (right).

After optimizing the algorithm on simulated images, real cross-sectional MR images of the CHIC fiducial frame were acquired in a Philips 3T MRI scanner. Representative results on real MR images of the fiducial are shown in Fig. 6.

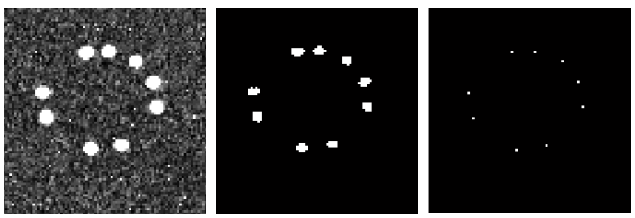

Figure 6. MR image of a tubular mesh cross-section of CHIC frame fiducial (left), filtered tubular mesh cross-section (center) and centroids of tube locations (right).

B. *Accuracy Assessment*

Registration accuracy of the CHIC fiducial frame was evaluated in three ways: 1) based on simulated images at known positions and orientations, 2) real 3T cross-sectional MR images, and 3) artificially reconstructed high resolution 3T MRI volume to provide a large number of cross-sectional images at known positions and orientations.

1. Simulation results

Four groups of simulation have been performed to evaluate the accuracy of the fiducial module – two groups for positioning error tests and two for orientation error tests. Based on simulated images like those shown in Fig. 5.

A group of normal sections with known distances as shown in Fig. 7 (top-left) was created. Cross-sections E-I with 5, 10, 20, 30 and 40mm to the end of the fiducial module are acquired from CAD model and used to create simulated images. The axial displacement error is shown in Fig. 7 (bottom-left). The maximum error is 0.130mm with a standard deviation is 0.039mm.

A group of tilted sections with known distances is tested to evaluate the positioning error. The cross-sections are shown in Fig. 7 (top-right). Cross-sections J-M have the same tilt angle of 30° relative to normal section and they are 10, 20, 30 and 40mm to the end of the fiducial module. The axial displacement error is shown in Fig. 7 (bottom-right). The maximum error is 1.015mm with a standard deviation of 0.247mm.

To evaluate orientation accuracy, a group of cross-sections A-D with known tilt angles of 15°, 30°, 45° and 60° is created as shown in Fig. 8 (top-left). The angular error of normal vector is shown in Fig. 8 (bottom-left). The maximum error is 0.456° with a standard deviation of 0.164°.

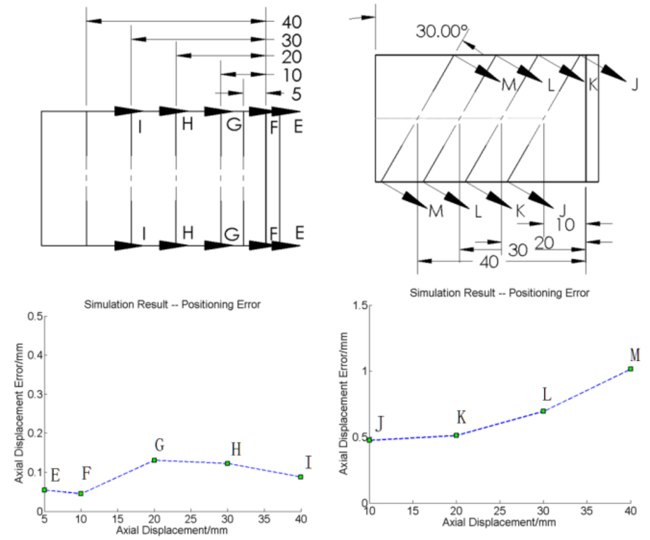

Figure 7. Simulation positioning accuracy evaluation: Normal sections with known distances (top-left) and their axial displacement error (bottom-left). Tilted sections with known distances (top-right) and their axial displacement error (bottom-right).

A group of normal sections with known twist angles was created to evaluate the twist angle error. The cross-sections of N-R with twist angles of 15°, 30°, 45°, 60° and 90° are shown in Fig. 8 (top-right). The twist angle error is shown in Fig. 8 (bottom-right). The maximum error is 0.032° with a standard deviation of 0.011°.

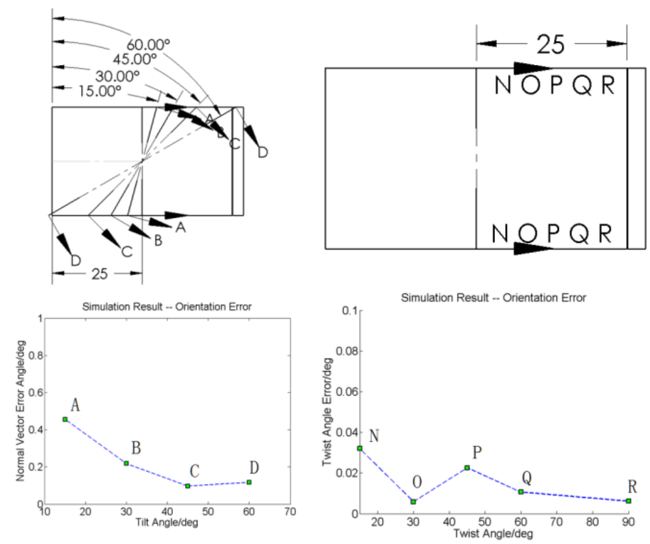

Figure 8. Simulation orientation accuracy evaluation: A group of cross-sections with known tilt angles (top-left) and their normal vector error (bottom-left). A group of normal sections with known twist angles (top-right) and their twist angle error (bottom-right).

2. Original MR image results

MR images of the fiducial module were acquired with a Philips 3T MRI scanner. The fiducial module was placed in the scanner at a random pose. The positioning and orientation accuracy are tested by taking a series of 14 images using a T2-weighted protocol, flip angle=45°, image size=256×256 pixels, pixel size=0.5×0.5mm, distance between slices=2mm. An assessment of precision of this set of images is shown in Table I.

TABLE I. ORIGINAL MR IMAGE PRECISION EVALUATION

	x	y	z	Tilt	Twist
RMS Error	0.620mm	0.144mm	0.269mm	0.086°	0.006°
Standard Deviation	0.166mm	0.166mm	0.280mm	0.089°	0.006°

3. Reformatted MR image results

To further evaluate reliability on a large set of images with known poses, a high resolution MRI volume was acquired. This volume was then artificially resliced to generate reformatted MR images of arbitrary, but known position and orientation. For a representative series of images reformatted with a tilt angle of 15° relative to original MR images and with the same image and pixel size, the precision results are shown in Table II.

TABLE II. REFORMATTED MRI POSITIONING AND ORIENTATION PRECISION TEST

	x	y	z	Tilt	Twist
RMS Error	0.111mm	0.091mm	0.312mm	0.006°	0.161°
Standard Deviation	0.114mm	0.094mm	0.311mm	0.006°	0.157°

IV. CONCLUSION

In this paper, we present a compact Cylindrical Helix Imaging Coordinate (CHIC) Registration Fiducial Frame with its mathematic model for 6-DOF registration from a single cross-sectional image in MRI. We evaluated the CHIC fiducial frame based on simulated images from CAD with added uniformly distributed white noise, and in actual MRI image. Two categories of registration errors were discussed: 1) position of image plane including x, y, z direction in fiducial frame and 2) orientation of image plane including tilt and twist angle. The approach proved to be robust to realistic noise in the input data. An important strength of CHIC frame with corresponding registration algorithm is the ability to determine 6-DOF pose from a single arbitrary oblique cross-sectional image, which is beneficial for image-guided applications based on real-time MR image data; accuracy can be further improved by utilizing multiple oblique slices together. The results shown are based on the prototype fiducial's configuration – it should be noted that the diameter, length, and pitch of the fiducial can be optimized for specific clinical applications. The immediate application that we are applying the fiducial to is MR image-guided stereotactic neurosurgery, and will be evaluated shortly in conjunction with the robot. The CHIC fiducial frame can serve a broad set of clinical uses and be affixed to a wide variety of instrument – it further may be configured for imaging modalities other than MRI by substituting the material in the tubular structures.

ACKNOWLEDGMENT

This work is supported in part by the Congressionally Directed Medical Research Programs Prostate Cancer Research Program (CDMRP PCRP) New Investigator Award W81XWH-09-1-0191 and Worcester Polytechnic Institute internal funds.

REFERENCES

[1] Cole, G., Pilitsis, J. and Fischer, G. S., "Design of a Robotic System for MRI-Guided Deep Brain Stimulation Electrode Placement," International Conference on Robotics and Automation - ICRA 2009, Kobe, Japan, 4450-4456 (2009)

[2] Su H., Zervas M., Cole G.A., Furlong C., Fischer G.S., "Real-time MRI-Guided Needle Placement Robot with Integrated Fiber Optic Force Sensing," International Conference on Robotics and Automation, Shanghai, China, pp 1583-1588 (2011)

[3] Krieger, A., Iordachita, I.I., Guion, P., Singh, A.K., Kaushal, A., Menard, C., Pinto, P.A., Camphausen, K., Fichtinger, G., Whitcomb, L.L., "An MRI-Compatible Robotic System With Hybrid Tracking for MRI-Guided Prostate Intervention," IEEE Transactions on Biomedical Engineering, vol.58, no.11, pp.3049-3060 (2011)

[4] Derbyshire, J. A., Wright, G. A., Henkelmann, R. M. and Hinks, S., "Dynamic scan-plane tracking using MR positioning monitoring," J. Magn. Reson. Imaging, 8, 924 – 932 (1998)

[5] Hillenbrand, C. M., Elgort, D. R., Wong, E. D., Reykowski, A., Wacker, F. K., Lewin, J. S. and Duerk, J. L., "Active device tracking and high-resolution intravascular MRI using a novel catheter-based, opposed-solenoid phased array coil," Magn. Reson. Med., 51, 668– 75 (2004)

[6] DiMaio, S., Samset, E., Fischer, G.S., Iordachita, I., Fichtinger, G., Jolesz, F. and Tempany, C., "Dynamic MRI Scan Plane Control for Passive Tracking of Instruments and Devices" MICCAI 2007, LNCS, vol. 4792, 50–58, Springer, Heidelberg (2007)

[7] Susil, R. C., Anderson, J.H. and Taylor, R.H., "A Single Image Registration Method for CT Guided Interventions," MICCAI 1999, Cambridge, England, LNCS 1679, 798-808 (1999)

[8] Lee, S., Fichtinger, G. and Chirikjian, G.S., "Numerical algorithms for spatial registration of line fiducials from cross-sectional images," Med. Phys., vol. 29, 1881–1891 (2002)

[9] Shang, W. and Fischer, G. S., "A High Accuracy Multi-Image Registration Method for Tracking MRI-Guided Robots," SPIE Medical Imaging, Image-Guided Procedures, Robotic Interventions, and Modeling Conference (2012)

[10] Jain, A., Mustufa, T., Zhou, Y., Burdette, E.C., Chirikjian, G., Fichtinger, G.: A robust fluoroscope tracking (ftrac) fiducial. Med. Phys. 32, 3185–3198 (2005)